

Holographic superconductor in the analytic hairy black hole

Yun Soo Myung ¹ and Chanyong Park ²

¹ *Institute of Basic Science and School of Computer Aided Science*

Inje University, Gimhae 621-749, Korea

² *Center for Quantum Spacetime (CQUeST), Sogang University, Seoul 121-742, Korea*

Abstract

We study the charged black hole of hyperbolic horizon with scalar hair (charged Martinez-Troncoso-Zanelli: CMTZ black hole) as a model of analytic hairy black hole for holographic superconductor. For this purpose, we investigate the second order phase transition between CMTZ and hyperbolic Reissner-Nordström-AdS (HRNAdS) black holes. However, this transition unlikely occur. As an analytic treatment for holographic superconductor, we develop superconductor in the bulk and superfluidity on the boundary using the CMTZ black hole below the critical temperature. The presence of charge destroys the condensates around the zero temperature, which is in accord with the thermodynamic analysis of the CMTZ black hole.

¹e-mail address: ysmyoung@inje.ac.kr

²e-mail address: cyong21@sogang.ac.kr

1 Introduction

Recently, the AdS/CFT correspondence has widely applied to investigating the superconductivity. In order to describe a superconductor, we introduce the temperature and charge density in the boundary field theory by adding a charged black hole [1, 2]. Then, we make a condensate through coupling of a charged scalar field ψ to a Maxwell field to define Cooper pair's operator and its charge density in the boundary theory. In these cases, the charged scalar field is minimally coupled to gravity. To represent the phase diagram for holographic superconductor, one supposes a system which admits black hole with scalar hair at low temperature, while at high temperature there is a black hole without hair, namely Reissner-Nordstöm-AdS₄ (FRNAdS) black hole with flat horizon. In all of these gravity constructions [3], the onset of the phase transition is triggered by a zero mode for the field that gives hair to the black hole. The FRNAdS black hole is unstable against the perturbation of the charged scalar because the effective mass $m_{\psi}^2 = m^2 + p^2 g^{tt} A_t^2$ of the scalar field becomes too negative [4]. Then, this perturbed scalar can develop a nontrivial profile without a ψ^4 -term to stabilize the run away direction of ψ . Superfluid phase transitions are associated with spontaneous symmetry breaking, while superconducting phase transitions are triggered by the Abelian-Higgs mechanism. Hence, superfluidity appears in the boundary field theory and superconductivity in the bulk gravity [5]. In terms of AdS/CFT picture, it implies that an instability of FRNAdS black hole to develop scalar hair is dual to a superfluid phase transition. Noting that the AdS/CFT correspondence maps classical gravity to a strongly interacting field theory, the correspondence opens a window onto strongly interacting superconductors and superfluids where the known BCS theory and weak coupling techniques are inapplicable [4]. Also, it is suggested that the endpoint of instability of RNAdS black hole with spherical horizon is a numerical hairy black hole [6].

In this direction, most of studies were being performed numerically. Solving the equations on the gravity side reduces to a set of nonlinear, coupled differential equations which could be solved on a computer. We call these as *numerical hairy black hole solutions*. This is so called because we could not obtain *an analytic hairy black hole solution* except a few cases: a complicated p -wave superconductor [7, 8] and a gapless superconductor of neutral MTZ black hole [9]. In the former, the dual boundary field theory has a vector rather than a scalar order parameter. On the other hand, in the latter, the charged scalar ϕ is conformally coupled to gravity and the scalar potential plays an essential role to develop scalar condensation. A second order phase transition between topological black hole and MTZ black hole [10] occurred at the critical temperature [11, 12]. It implies that below

the critical temperature, the MTZ black hole acquires its scalar hair, while an electromagnetic perturbation determines the conductivity and then, the superfluid density of the boundary theory.

At this stage, we would like to mention the difference on the mechanism of condensation of the scalar field. In the case of a FRNAdS black hole, the scalar field condensates because the Abelian-Higgs mechanism was operating without ψ^4 -term [13], while for the MTZ black hole, the condensation of the scalar was made by conformally coupling to gravity and the presence of ϕ^4 -term in the potential. The conformal coupling provides a single effective mass $m_\phi^2 = -1/l^2$, which is larger than the Breitenlohner-Freedman bound, $m_{\text{BF}}^2 = -9/4l^2$ in the AdS₄ spacetime [14]. Importantly, the presence of ϕ^4 -term is essential for developing an exact scalar hair in the hyperbolic horizon [15]. It is worth to note that the presence of potential and horizon topology gives rise to an exact scalar hair on the gravity side. Hence, it is considered as an exact gravity dual of a gapless superconductor [9]. However, the MTZ black hole is considered as a probe limit because it belongs to a neutral black hole.

Fortunately, the charged MTZ (CMTZ) black hole was found with scalar hair when the coefficient α of ϕ^4 -term is between 0 and $2\pi G/3l^2$ [15], where the upper bound corresponds to the MTZ black hole [10] and the lower bound is not allowed. Hence, it is very interesting to investigate whether or not a pair of the CMTZ and HRNAdS black holes provides a second order phase transition. It was proposed that this transition is likely possible to occur for a special case of $\tilde{q}^2 = -G\mu^2$ HRNAdS black hole [16]. If this pair is the case, it would provide a really analytic gravity dual to a holographic superconductor. However, the previous analysis might be wrong because the $\tilde{q}^2 = -G\mu^2$ case is not allowed in the HRNAdS black holes. Moreover, the entropy of the CMTZ black hole is not the Bekenstein-Hawking entropy but it should be obtained using either the Euclidean action approach or the Wald method because of the conformal coupling of scalar to gravity. In this case, the negative entropy appears [15], which in turn confines the free energy to restricted ranges, depending on the charge q . Therefore, the presumed second order phase transition unlikely occurs between CMTZ and HRNAdS black holes.

On the other hand, we have an analytic charged black hole with scalar hair, even though the corresponding black hole without scalar hair is not clearly known. In this case, we would like to make a progress on the superfluidity on the boundary by studying the superconductivity on the gravity side. This situation is opposite to a case of numerical hairy black holes that the charged black holes without scalar hair were known explicitly, while the charged black holes with scalar hair were found numerically.

The organization of this work is as follows. Section 2 is devoted to reviewing the

hyperbolic Reissner-Nordström-AdS₄ (HRNAdS) black hole as charged black hole without scalar hair. We study the CMTZ black hole as the charged black hole with scalar hair in section 3. We investigate superconductivity and superfluidity for the CMTZ black hole thoroughly in section 4. Finally, we discuss our results by comparing the known results.

2 HRNAdS black holes

Topological black holes in asymptotically anti-de Sitter spacetimes were first found in three and four dimensions [17]. Their black hole horizons are Einstein spaces of spherical, hyperbolic, and flat curvature for higher dimensions more than three [18, 19]. The standard equilibrium and off-equilibrium thermodynamic approaches to these black holes are possible to show that they are treated as the extended thermodynamic systems, even though their horizons are not spherical.

We start with the Einstein-Maxwell action

$$I_4[g, A_\mu] = \int d^4x \sqrt{-g} \left[\frac{R - 2\Lambda}{16\pi G} - \frac{1}{16\pi} F^{\mu\nu} F_{\mu\nu} \right] \quad (1)$$

where $\Lambda = -3/l^2$ with l is the curvature radius of AdS₄ spacetimes. For $A = 0$ case, we obtain the action for the four dimensional topological black hole. For $A = -\frac{\tilde{q}}{\rho} dt$, the charged topological black hole (CTBH) in AdS₄ spacetimes are given by

$$ds_{\text{CTBH}}^2 = g_{\mu\nu} dx^\mu dx^\nu = -f_k(\rho) dt^2 + \frac{1}{f_k(\rho)} d\rho^2 + \rho^2 d\Sigma_k^2, \quad (2)$$

where the metric function $f_k(\rho)$ is given by

$$f_k(\rho) = k + \frac{\rho^2}{l^2} - \frac{2G\mu}{\rho} + \frac{G\tilde{q}^2}{\rho^2} \quad (3)$$

where μ and \tilde{q} are related to the mass parameter and charge of black hole, respectively. For $\tilde{q} = 0$, the above reduces to topological black hole (TBH). For $k = -1$ and $\tilde{q}^2 = -G\mu^2$, the metric function leads to the same form as (21) for the CMTZ black hole. However, this case is not allowed because $\tilde{q}^2 = -G\mu^2$ implies an imaginary charge ($\tilde{q} = i\sqrt{G}\mu$). $d\Sigma_k^2$ describes the 2D horizon geometry with a constant curvature as Einstein space

$$d\Sigma_k^2 = d\theta^2 + p_k^2(\theta) d\varphi^2 \equiv h_{ij}^k dx^i dx^j, \quad (4)$$

where $p_k(\theta)$ is given by

$$p_0(\theta) = \theta, \quad p_1(\theta) = \sin \theta, \quad p_{-1}(\theta) = \sinh \theta. \quad (5)$$

For $k = -1$, one has that $\theta \geq 0$ and $0 \leq \varphi \leq 2\pi$ denote the coordinates of the hyperbolic space H^2 . Here we define $k=1, 0$, and -1 cases as the Reissner-Norström-AdS black hole (RNAdS), flat RNAdS black hole (FRNAdS), and hyperbolic RNAdS (HRNAdS) black holes [20], respectively. It is easy to check that the metric (2) satisfies

$$R = 4\Lambda, \quad (6)$$

when the horizon is an Einstein space

$$R_{ij} = kh_{ij}^k. \quad (7)$$

In this work, we are interested in the negative curvature with $k = -1$ only. Then, the horizon space is a hyperbolic manifold of $\Sigma_{k=-1} = H^2/\Gamma$, where H^2 is 2D hyperbolic space and Γ is a freely acting discrete subgroup of the isometry group $O(2, 1)$ of H^2 [21]. This manifold has genus $g \geq 2$ and its area is given by $\sigma = 4\pi(g - 1)$. For numerical calculations, we choose $g = 2$, $\sigma = 4\pi$, $G = 1$, and $l = 1$. The boundary has the metric

$$ds_{\partial}^2 = -dt^2 + l^2 d\sigma^2 \quad (8)$$

which is a hyperbolic manifold of radius l and its curvature is negative as $-1/l$.

3 CMTZ black holes

In order to understand the role of scalar and its potential well, it would be better to start with the conformally coupled action [9]

$$I_4[g, \phi, A_\mu] = \int d^4x \sqrt{-g} \left[\frac{R - 2\Lambda}{16\pi G} - (D_\mu \phi)^* (D^\mu \phi) - \frac{1}{6} R \phi \phi^* - 4\alpha (\phi \phi^*)^2 - \frac{1}{16\pi} F^{\mu\nu} F_{\mu\nu} \right], \quad (9)$$

where a conformally charged coupled scalar ϕ appears with a conventional potential term $\alpha(\phi\phi^*)^2$ and

$$D_\mu \phi \equiv \partial_\mu \phi + ipA_\mu \phi. \quad (10)$$

We note the mass dimensions of $[\phi] = [\phi^*] = [A_\mu] = 1$. For $\phi = 0$, one has the action (1) for HRNAdS black hole. We note that α is an arbitrary coupling constant, but it was given by $\alpha = 2\pi G/3l^2$ for the MTZ black hole without Maxwell field [10]. The equations of motion are given by

$$G_{\mu\nu} + \Lambda g_{\mu\nu} = 8\pi G (T_{\mu\nu}^\phi + T_{\mu\nu}^{em}), \quad (11)$$

$$\frac{1}{\sqrt{-g}} D_\mu (\sqrt{-g} D^\mu \phi) = \frac{1}{6} R \phi + 8\alpha \phi^2 \phi^*, \quad (12)$$

$$\nabla_\nu F^{\mu\nu} = 4\pi J^\mu, \quad (13)$$

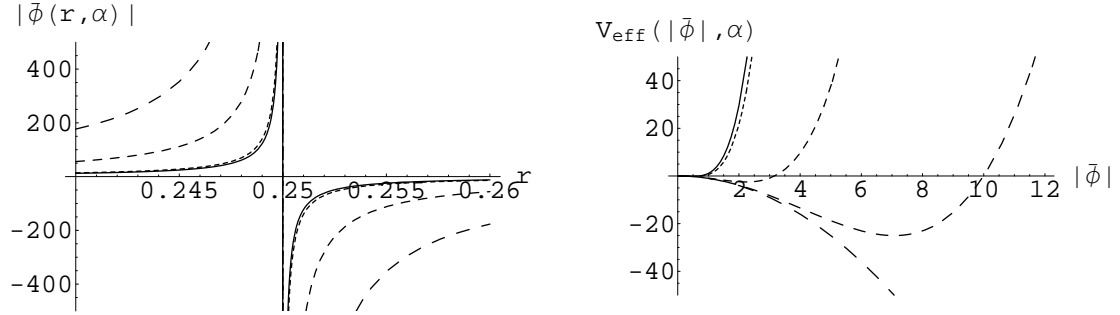


Figure 1: Modulus of scalar $|\bar{\phi}(r, \alpha, \mu)|$ with $\mu = -\frac{1}{4}$ for $\alpha = 2\pi G/3, 1.6, 0.1, 0.01$ and its effective potentials $V_{eff}(|\bar{\phi}|, \alpha)$ for $\alpha = 2\pi G/3, 1.6, 0.1, 0.01, 0$ from top to bottom. We observe that a scalar singularity at $r = -G\mu = 1/4$ exists for all α , which is responsible for scalar hair in the CMTZ black holes.

with

$$T_{\mu\nu}^{\phi} = [D_{\mu}\phi(D_{\nu}\phi)^* + D_{\nu}\phi(D_{\mu}\phi)^*] - g_{\mu\nu}(D_{\beta}\phi)^*(D^{\beta}\phi) + \frac{1}{3}[g_{\mu\nu}\nabla^2 - \nabla_{\mu}\nabla_{\nu} + G_{\mu\nu}]\phi\phi^* - 4\alpha(\phi\phi^*)^2g_{\mu\nu}, \quad (14)$$

and

$$T_{\mu\nu}^{em} = \frac{1}{4\pi}(F_{\mu\beta}F_{\nu}^{\beta} - \frac{1}{4}g_{\mu\nu}F^2), \quad J_{\mu} = -ip(\phi^*D_{\mu}\phi - \text{c.c.}). \quad (15)$$

Since the scalar field is conformally coupled, the total energy-momentum tensor is traceless. The Ricci curvature scalar is constant

$$\bar{R} = 4\Lambda. \quad (16)$$

Since Eq. (12) can be rewritten as

$$\frac{1}{\sqrt{-g}}D_{\mu}(\sqrt{-g}D^{\mu}\phi) = \frac{\partial V_{eff}}{\partial\phi^*}, \quad (17)$$

it implies the form of an effective potential

$$V_{eff}(\phi) = \frac{1}{6}\bar{R}\phi\phi^* + 4\alpha(\phi\phi^*)^2. \quad (18)$$

Taking the scalar to be the modulus

$$\phi \rightarrow \frac{|\phi|}{\sqrt{2}} \quad (19)$$

together with $p \simeq 0$ ¹, all equations (11)-(13) reduce to those in the neutral scalar coupled system. Then, the solution is given by the CMTZ black hole

$$ds_M^2 = -f_M(r)dt^2 + \frac{dr^2}{f_M(r)} + r^2 d\Sigma_{k=-1}^2 \quad (20)$$

where the metric function $f_M(r)$ is given by

$$f_M(r) = \frac{r^2}{l^2} - \left(1 + \frac{G\mu}{r}\right)^2. \quad (21)$$

The modulus of scalar field and the electromagnetic potential take the forms, respectively,

$$|\bar{\phi}(r, \alpha, \mu)| = -\sqrt{\frac{1}{2\alpha l^2} \frac{G\mu}{r + G\mu}}, \quad \bar{A}_t = -\frac{q}{r}. \quad (22)$$

As is shown in Fig. 1, the modulus of scalar and its potential are depicted for $\alpha = \frac{2\pi G}{3l^2}, 1.6, 0.1, 0.01, 0$. The modulus of scalar field has a simple pole at $r = -G\mu$ for all α only if μ is negative, while shapes of its potential are drastically changed from $\alpha = 0$, $V_{\text{eff}}(\phi) = -|\bar{\phi}|^2/l^2$ to $\alpha \neq 0$ case of $V_{\text{eff}} = -|\bar{\phi}|^2/l^2 + \alpha|\bar{\phi}|^4$. This makes a difference between $\alpha = 0$ and $\alpha \neq 0$. $\alpha = \frac{2\pi G}{3l^2}$ corresponds to the neutral MTZ black hole. We note here that the singularity of modulus at $r = -G\mu$ is essential for having the CMTZ black hole dressed by scalar field and electric charge.

Importantly, the charge is no longer an independent parameter and thus it should be determined by the relation

$$q^2 = G\mu^2 \left(-1 + \frac{2\pi G}{3\alpha l^2} \right) \quad (23)$$

which determines, from the condition of $q^2 \geq 0$, the lower and upper bound for the coupling constant α as

$$0 < \alpha \leq \frac{2\pi G}{3l^2}. \quad (24)$$

Because of the above bound, it is convenient to express α in terms of μ and q

$$\alpha(\mu, q) = \frac{2\pi G^2 \mu^2}{3l^2(G\mu^2 + q^2)} \quad (25)$$

which means that “ μ and q ” are two conserved quantities for the CMTZ black hole.

¹Precisely, for $p \neq 0$, the CMTZ black hole solution is not an exact solution to (11)-(13). Actually, we could not obtain the exact complex scalar hairy black hole including the nonzero p . In this work, we use the CMTZ black hole to investigate the density dependence of the dual condensed matter system in the small p limit.

In the case of positive mass $\mu > 0$, analytic hairy black holes possess a single event horizon located at

$$r_+ = \frac{l}{2} \left(1 + \sqrt{1 + \frac{4G\mu}{l}} \right) \quad (26)$$

which satisfies $r_+ > l$ and the scalar is regular everywhere. However, this case has nothing to do with developing holographic superconductor. On the other hand, an important feature of the hairy black hole is that a complicated horizon structure appears for $-l/4G < \mu < 0$. The hairy black hole has three horizons located at

$$r_{\pm} = \frac{l}{2} \left(1 \pm \sqrt{1 + \frac{4G\mu}{l}} \right), \quad r_{--} = \frac{l}{2} \left(-1 + \sqrt{1 - \frac{4G\mu}{l}} \right) \quad (27)$$

which satisfy an inequality

$$0 < r_{--} < -G\mu < r_- < \frac{l}{2} < r_+. \quad (28)$$

The outermost r_+ and innermost r_{--} horizons are event horizons and thus one may say that this metric describes “a black hole in the black hole”. The causal structure of Penrose diagram was constructed in Ref.[15].

Thermodynamic quantities of the CMTZ are given by Hawking temperature $T_M = \frac{f'_M(r_+)}{4\pi}$, mass $M_M = \frac{\sigma}{4\pi}\mu$, heat capacity $C_M = \left(\frac{\partial M_M}{\partial T_M} \right)_Q$ by [10, 11, 12]

$$T_M(r_+) = \frac{1}{2\pi l} \left[\frac{2r_+}{l} - 1 \right], \quad M_M(r_+) = \frac{\sigma r_+}{4\pi G} \left(\frac{r_+}{l} - 1 \right), \quad C_M(r_+) = \frac{\sigma l^2}{4G} \left(\frac{2r_+}{l} - 1 \right), \quad (29)$$

which are the same quantities as in the MTZ black hole. Here we observe a linear relation between temperature and heat capacity

$$T_M = \frac{2G}{\pi\sigma l^3} C_M = \frac{2G}{\pi\sigma l^3} S_{\text{MTZ}} \quad (30)$$

with the entropy for the MTZ black hole

$$S_{\text{MTZ}}(r_+) = \frac{\sigma l^2}{4G} \left(\frac{2r_+}{l} - 1 \right). \quad (31)$$

However, since the conformal coupling term appears in the action, the entropy should be obtained by making use of the Euclidean action approach [15] and the Wald method [22] as

$$S_M(r_+, q) = \frac{\sigma r_+^2}{4\tilde{G}} = \frac{\sigma l^2}{4G} \left(\frac{2r_+}{l} - 1 - \frac{Gq^2}{r_+^2} \right), \quad (32)$$

where an effective Newtonian constant at the event horizon is given by

$$\frac{1}{\tilde{G}} = \frac{1}{G} \left(1 - \frac{4\pi G}{3} |\bar{\phi}|^2 \right). \quad (33)$$

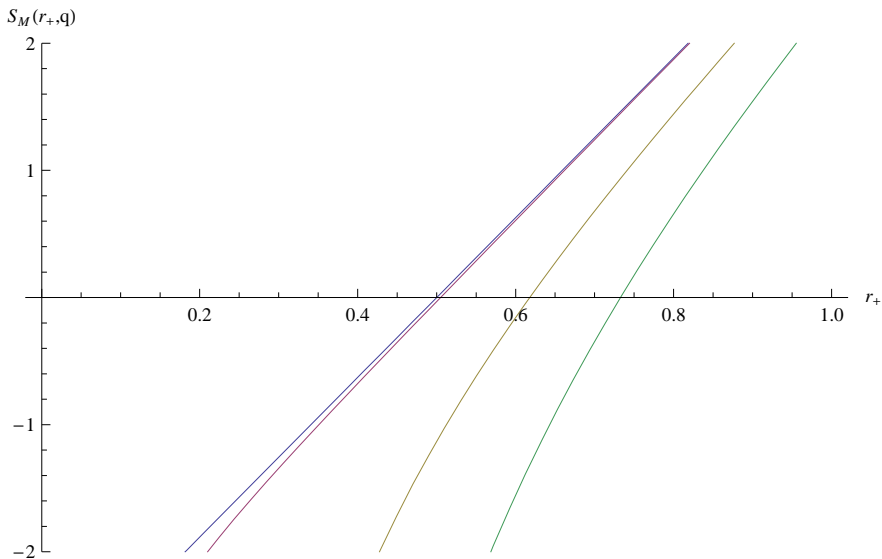


Figure 2: Entropy graph: the allowed regions for positive entropy $S_M(r_+, q)$ with $q = 0, 0.05, 0.3, 0.5$ from top to bottom. The first case (top) corresponds to the MTZ black hole with $q = 0$: $0.5 \leq r_+ < \infty$. The permitted regions gets narrow and narrow as q increases from 0.05 to 0.5: $0.51 \leq r_+ < \infty$ for $q = 0.05$, $0.62 \leq r_+ < \infty$ for $q = 0.3$, and $0.73 \leq r_+ < \infty$ for $q = 0.5$ (bottom).

The positivity of entropy $S_M \geq 0$ requires a bound

$$r_+^2 \left(\frac{2r_+}{l} - 1 \right) \geq Gq^2. \quad (34)$$

It requires lower bounds for being the positive entropy. As is depicted in Fig. 2, the allowed region depends on the charge q critically. The MTZ black hole corresponds to the largest region between $l/2 \leq r_+ < \infty$. However, the permitted region gets narrow and narrow as the charge q increases. As $q \rightarrow \infty$, the allowed region approaches a point at $r_+ = \infty$ and thus, we could not define the entropy. We note that the first law of thermodynamics $dM_M = T_M dS_M - \Phi dQ$ with $\Phi = -q/r_+$ and $Q = \sigma q/4\pi$ is no longer satisfied for the CMTZ black hole, in contrast to the MTZ black hole with $q = 0$.

We would like to mention the thermodynamic property of extremal CMTZ black hole since it may describe the zero temperature limit of the holographic superconductivity [4]. We note that the temperature and heat capacity at the extremal point $r_+ = r_e = l/2$ take the form

$$T_M^e = C_M^e = 0. \quad (35)$$

The entropy for extremal CMTZ black hole is always negative as is shown by

$$S_M^e\left(\frac{l}{2}, q\right) = -\sigma q^2 \leq 0 \quad (36)$$

for $q \geq 0$ in (24). The lower equality represents the zero entropy of extremal MTZ black hole. Hence, all allowed region for r_+ depending q exclude their extremal black holes at $r = r_e$.

The free energy is a key quantity to see the second order phase transition between HRNAdS and CMTZ black holes. Actually, to study the first order phase transition as the Hawking-Page transition [23], one requires the heat capacity and free energy because it describes a phase transition from a hot gas, via small unstable black hole with negative heat capacity, to large stable black hole with positive heat capacity in AdS₄ spacetimes [24]. However, the second order phase transition occurs between two different black holes with positive heat capacity. Thus, it suggests that the heat capacity does not play the role in determining the second order phase transition.

In order to see whether the second order phase transition occurs between HRNAdS and CMTZ black holes, we note that the free energy for CMTZ black hole defined by

$$F_M = M_M - T_M S_M + \Phi Q \quad (37)$$

takes a form

$$F_M(r_+, q) = \frac{\sigma r_+}{4\pi G} \left(\frac{r_+}{l} - 1\right) - \frac{\sigma(2r_+ - l)}{8\pi G} \left(\frac{2r_+}{l} - 1\right) - \frac{\sigma l q^2}{8\pi r_+^2}. \quad (38)$$

Here we easily check that for $q = 0$, F_M reproduces the free energy for the MTZ black hole

$$F_{\text{MTZ}}(r_+) = -\frac{\sigma}{8\pi G} \left(\frac{2r_+^2}{l} - 2r_+ + l\right). \quad (39)$$

In order to implement the phase transition to the corresponding black hole without scalar hair, we need the free energy without any restriction. However, it is clear that the bound (34) puts restriction on the free energy. The onset of black hole charge disturbs a transition to the corresponding black hole without scalar hair. A promising case is the probe limit that a pair of neutral black holes of MTZ and TBH provides the second order phase transition [11, 12].

Finally, we argue that a q -dependent free energy is not suitable (sufficient) for studying a transition to the corresponding black hole without scalar hair. In the next section, we will show explicitly that the onset of charge density on the boundary disturbs making a solid superconducting and superfluidity phase.

4 Gapless superconductivity

We remind that an analytic hairy black hole was known. Even though the corresponding black hole without scalar hair is unknown, we wish to explore the superfluidity on the boundary by studying the superconductivity on the gravity side. This situation is opposite to the numerical hairy black hole case that the charged black hole without scalar hair is known, whereas the charged black hole with scalar hair is found numerically. In that case, an instability of scalar field near (at) the event horizon develops the scalar hair and thus, the superfluidity on the boundary.

Below the critical temperature defined by $T_0 = \frac{1}{2\pi l}$, the CMTZ black hole solution acquires a scalar hair and thus, a condensation forms. Near the boundary, the modulus of scalar field could be expanded as

$$|\bar{\phi}| = \frac{\phi^{(1)}}{r} + \frac{\phi^{(2)}}{r^2} + \dots, \quad (40)$$

where

$$\phi^{(1)} = -\sqrt{\frac{1}{2\alpha l^2}} G\mu \quad \text{and} \quad \phi^{(2)} = \sqrt{\frac{1}{2\alpha l^2}} G^2\mu^2. \quad (41)$$

Two non-vanishing coefficients correspond to the condensates of two dual scalar operator \mathcal{O}_i ($i = 1, 2$), respectively,

$$\langle \mathcal{O}_i \rangle = \sqrt{2}\phi^{(i)}, \quad i = 1, 2. \quad (42)$$

We emphasize that unlike the numerical hairy black hole, the existence of two condensates does not always imply an instability of CMTZ black hole. As was in (29), one notes that this black hole is thermodynamically stable when α approaches its neutral value ($\alpha \rightarrow \frac{2\pi G}{3l^2}$, equivalently $q \rightarrow 0$) because $C_M > 0$ and $F_M(r_+, q \rightarrow 0) = F_{\text{MTZ}} < 0$ in (39). We express α in (25) in terms of q and

$$\mu(T_M) = -\frac{T_0^2 - T_M^2}{8\pi G T_0^3} \quad (43)$$

through $r_+ = \pi l^2(T_M + T_0)$. Furthermore, substituting these into (41) leads to two condensates which take the forms

$$\langle \mathcal{O}_1 \rangle = \sqrt{\frac{3}{2\pi}} \sqrt{q^2 + \frac{(T_0^2 - T_M^2)^2}{64\pi^2 G T_0^6}}, \quad (44)$$

$$\langle \mathcal{O}_2 \rangle = \frac{\sqrt{3}(T_0^2 - T_M^2)}{8\sqrt{2} \pi^{3/2} T_0^3} \sqrt{q^2 + \frac{(T_0^2 - T_M^2)^2}{64\pi^2 G T_0^6}}, \quad (45)$$

which for $q = 0$, reduce to the same expressions found in Ref. [9]. When q is turned on, the first condensate $\langle \mathcal{O}_1 \rangle$ does not go to zero at the critical temperature $T_M = T_0$. Since

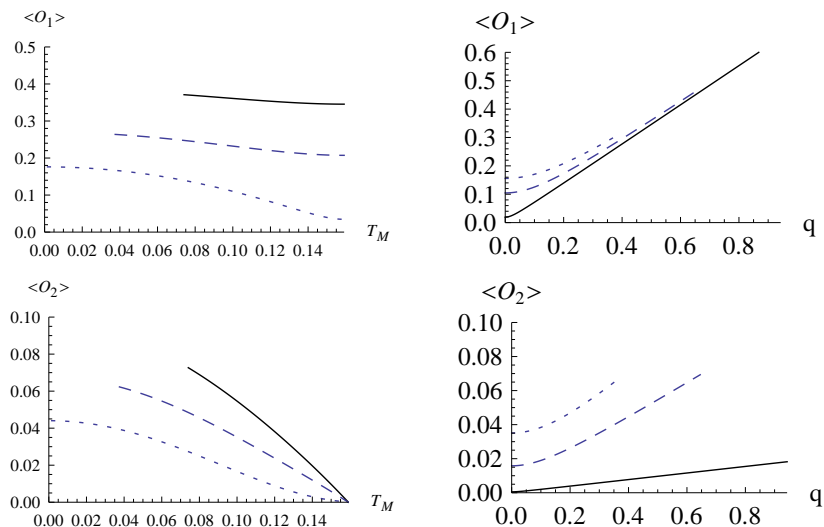


Figure 3: The condensates $\langle \mathcal{O}_1 \rangle$ and $\langle \mathcal{O}_2 \rangle$ as functions of temperature T_M and charge density q . Left column: condensates as functions of T_M are plotted for $q = 0.5$ (solid), 0.3 (dashed) and 0.05 (dotted). Right column: condensates as functions of q are shown for $T_M = 0.15$ (solid), 0.1 (dashed) and 0.05 (dotted).

the first condensate does not become zero at the critical temperature, unlike the MTZ black hole, the second order phase transition between HRNAdS and CMTZ black holes may not occur. This is consistent with the thermodynamic analysis of the black hole in the previous section. Moreover, near the critical temperature, two condensate behave like

$$\begin{aligned} \langle \mathcal{O}_1 \rangle &\simeq \sqrt{\frac{3}{2\pi}} q, \\ \langle \mathcal{O}_2 \rangle &\simeq \frac{\sqrt{3} q}{4\sqrt{2} \pi^{3/2} T_0} \left(1 - \frac{T_M}{T_0}\right). \end{aligned} \quad (46)$$

Comparing these critical exponents with those of the MTZ black hole [9], the black hole charge q which corresponds to the charge density on the boundary field theory decreases the critical exponents c_i defined by $\langle \mathcal{O}_i \rangle \simeq \left(1 - \frac{T_M}{T_0}\right)^{c_i}$: $c_1 = 1 \rightarrow 0$ and $c_2 = 2 \rightarrow 1$. In Fig. 3, we plot two condensates (44) and (45) as functions of T_M and q . As shown in these figures, we find that the condensate decreases as the temperature increases. On the other hand, condensates increase as the charge density q increases. At the critical temperature, $\langle \mathcal{O}_2 \rangle$ goes to zero irrespective of the charge density, whereas $\langle \mathcal{O}_1 \rangle$ remains as a constant value for nonzero q . From this observation and (46), we find that the charge density q significantly changes the condensates.

Now we are in a position to investigate the electric conductivity. For this purpose, we

perform the electromagnetic perturbations around the CMTZ hyperbolically symmetric background only by considering

$$A_\mu = \bar{A}_\mu + a_\mu. \quad (47)$$

Linearizing (13), a s-wave gauge field fluctuation satisfies

$$f_M \partial_r (f_M \partial_r a_w) + \left(w^2 - p^2 |\bar{\phi}|^2 f_M \right) a_w = 0, \quad (48)$$

where p is a charge of the complex scalar field and we use the fourier transformation to define a_w

$$a_\theta(t, r) = \int \frac{dw}{2\pi} e^{-iwt} a_w(r). \quad (49)$$

In deriving (48), we used the wave function of the lowest harmonic which corresponds to the lowest eigenvalue in the compact hyperbolic space $\Sigma_{k=-1} = H^2/\Gamma$ given by $\xi^2 + 1/4 = 0$. We note that the gauge perturbation in φ -direction $a_\varphi(t, r)$ can be also described by (48) because we are working in the hyperbolically symmetric background. We could not solve (48) analytically. We may solve this equation for weak coupling p^2 using the perturbation theory. In order to get a solution near horizon, we introduce the tortoise coordinate as

$$r^* = - \int_r^\infty \frac{d\tilde{r}}{f_M(\tilde{r})}, \quad (50)$$

which satisfies

$$\frac{dr^*}{dr} = \frac{1}{f_M}. \quad (51)$$

Then, Eq. (48) leads to the Schrödinger-type equation

$$\frac{d^2 a_w}{dr^{*2}} + \left(w^2 - p^2 |\bar{\phi}|^2 f_M \right) a_w = 0. \quad (52)$$

Since f_M is nearly zero near the horizon, we can easily solve the above equation. An incoming wave near the horizon is given by

$$a_w^\leftarrow = e^{-iwr^*}. \quad (53)$$

For small p^2 regime, one keeps the first order perturbation expansion of p^2 . We find that near the boundary, a_w is given approximately by

$$a_w = e^{-iwr^*} + \frac{p^2}{2iw} e^{iwr^*} \int_{r_+}^r d\tilde{r} |\bar{\phi}|^2 e^{-2iwr^*} - \frac{p^2}{2iw} e^{-iwr^*} \int_{r_+}^r d\tilde{r} |\bar{\phi}|^2 + \dots \quad (54)$$

Expanding a_w in the large r , we obtain

$$a_w = a_w^{(0)} + \frac{a_w^{(1)}}{r} + \dots \quad (55)$$

with

$$\begin{aligned} a_w^{(0)} &= 1 + \frac{p^2}{2iw} \int_{r_+}^{\infty} d\tilde{r} |\bar{\phi}|^2 (e^{-2iwr^*} - 1), \\ a_w^{(1)} &= iw - \frac{p^2}{2} \int_{r_+}^{\infty} d\tilde{r} |\bar{\phi}|^2 (e^{-2iwr^*} + 1). \end{aligned} \quad (56)$$

Then, we read off the conductivity to the first order in p^2 as

$$\sigma(w) = \frac{a_w^{(1)}}{iwa_w^{(0)}} = 1 - \frac{p^2}{iw} \int_{r_+}^{\infty} dr |\bar{\phi}|^2 e^{-2iwr^*}. \quad (57)$$

We note that the superfluid density n_s is given by the coefficient of the delta function of the real part of conductivity [9]

$$Re[\sigma(w)] \sim \pi n_s \delta(w), \quad (58)$$

which is also the coefficient of the pole in the imaginary part

$$Im[\sigma(w)] \sim \frac{n_s}{w} \quad \text{for } w \rightarrow 0. \quad (59)$$

Then, n_s becomes

$$n_s = \frac{p^2}{2\alpha l^2} \frac{G^2 \mu^2}{r_+ + G\mu}. \quad (60)$$

Using the temperature T_M and density q , the superfluid density for small p^2 can be rewritten as

$$n_s^\alpha = \frac{6p^2 T_0^3}{(T_0 + T_M)^2} \left(q^2 + \frac{(T_0^2 - T_M^2)^2}{64\pi^2 G T_0^6} \right). \quad (61)$$

In the limit of $q^2 \rightarrow 0$, we find that n_s^q reduces to n_s of the probe limit in Ref. [9]. Also, we note that near the zero temperature $T_M = 0$,

$$n_s^q(0) - n_s^q(T_M) \simeq T_M \quad (62)$$

which matches the low temperature behavior of heat capacity in (30).

5 Discussion

First of all, we would like to mention that the exact gravity dual of a gapless superconductor based on the TBH-MTZ black holes [9] was considered as a probe limit-description of holographic superconductor because these black hole belongs to neutral black holes without charge. We have studied the CMTZ black hole as a model of analytic hairy black

hole for holographic superconductor. This situation is opposite to a case of numerical hairy black holes that the charged black holes without scalar hair were known explicitly, while the charged black holes with scalar hair were found numerically. In this work, we have reanalyzed the phase transition between HRNAdS and CMTZ black holes. However, this transition unlikely occur, which means that HRNAdS black holes may not be the corresponding black hole without scalar hair. We note that a special transition between HRNAdS with $\tilde{q} = i\sqrt{G}\mu$ and CMTZ black hole with $q = i\sqrt{G}\mu$ [16] is not allowed because this channel is beyond the real transition. Explicitly, the presence of black hole charge affects thermodynamics of CMTZ black holes drastically: changing from $\alpha = \frac{2\pi G}{3l^2}$ to $\alpha = 0$ means increasing of charge from $q = 0$ to $q = \infty$. This is mainly because there exists some restriction on defining the entropy and free energy of CMTZ black hole due to the black hole charge q . The onset of black hole charge disturbs a transition to the corresponding black hole without scalar hair. An exceptional case is a pair of neutral black holes of MTZ and TBH where the second order phase transition was well established [11, 12].

As an analytic treatment for holographic superconductor, we have developed superconductor in the bulk and superfluidity on the boundary using the CMTZ black hole below the critical temperature. This might provide an analytic hairy black hole to study the holographic superconductor. It was shown that the presence of charge density destroys the condensates, which is in accord with the thermodynamic analysis of the CMTZ black hole. At the critical temperature $T = T_0$, $\langle \mathcal{O}_2 \rangle$ goes to zero, irrespective of the charge density q , whereas $\langle \mathcal{O}_1 \rangle$ remains as a constant value for nonzero q . Hence, we find that the charge density q affects the onset of the superconductivity.

Finally, we consider the zero temperature limit of holographic superconductor [25]. As was shown in black hole thermodynamics, each allowed region for free energy excludes the extremal black hole at the zero temperature $T_M(r_e) = 0$ except the MTZ black hole. The entropies of extremal CMTZ black holes all are negative (see (36)) which is unacceptable for black hole thermodynamics, while the entropy of extremal MTZ black hole is zero [26]. We observe that similar results for the conductivity depending on the charge density were found in the Horowitz-Roberts model [26] and Ref.[27].

In conclusion, we have shown that the onset of charge density on the boundary disturbs making a solid superfluidity phase by studying an analytic hairy solution of CMTZ black hole. Hence, it seems difficult to find an exact hairy black hole which describes the holographic superconductor and its corresponding black hole without scalar hair, compared to numerical hairy black holes.

Acknowledgments

Y. Myung was in part supported by Basic Science Research Program through the National Research Foundation (NRF) of Korea funded by the Ministry of Education, Science and Technology (2011-0027293) and the NRF grant funded by the Korea government (MEST) through the Center for Quantum Spacetime (CQUeST) of Sogang University with grant number 2005-0049409. C. Park was supported by the NRF grant funded by the Korea government (MEST) through the Center for Quantum Spacetime (CQUeST) of Sogang University with grant number 2005-0049409.

References

- [1] S. S. Gubser, Phys. Rev. D **78**, 065034 (2008) [arXiv:0801.2977 [hep-th]].
- [2] S. A. Hartnoll, C. P. Herzog and G. T. Horowitz, Phys. Rev. Lett. **101**, 031601 (2008) [arXiv:0803.3295 [hep-th]].
- [3] S. A. Hartnoll, Class. Quant. Grav. **26**, 224002 (2009) [arXiv:0903.3246 [hep-th]].
- [4] G. T. Horowitz, arXiv:1002.1722 [hep-th].
- [5] C. P. Herzog, J. Phys. A **42**, 343001 (2009) [arXiv:0904.1975 [hep-th]].
- [6] K. Maeda, S. Fujii and J. i. Koga, Phys. Rev. D **81**, 124020 (2010) [arXiv:1003.2689 [gr-qc]].
- [7] P. Basu, J. He, A. Mukherjee and H. H. Shieh, JHEP **0911**, 070 (2009) [arXiv:0810.3970 [hep-th]].
- [8] C. P. Herzog and S. S. Pufu, JHEP **0904**, 126 (2009) [arXiv:0902.0409 [hep-th]].
- [9] G. Koutsoumbas, E. Papantonopoulos and G. Siopsis, JHEP **0907**, 026 (2009) [arXiv:0902.0733 [hep-th]].
- [10] C. Martinez, R. Troncoso and J. Zanelli, Phys. Rev. D **70**, 084035 (2004).
- [11] G. Koutsoumbas, S. Musiri, E. Papantonopoulos and G. Siopsis, JHEP **0610**, 006 (2006) [arXiv:hep-th/0606096].
- [12] Y. S. Myung, Phys. Lett. B **663**, 111 (2008) [arXiv:0801.2434 [hep-th]].

- [13] C. P. Herzog, Phys. Rev. D **81**, 126009 (2010) [arXiv:1003.3278 [hep-th]].
- [14] P. Breitenlohner and D. Z. Freedman, Annals Phys. **144**, 249 (1982).
- [15] C. Martinez, J. P. Staforelli and R. Troncoso, Phys. Rev. D **74**, 044028 (2006) [arXiv:hep-th/0512022].
- [16] G. Koutsoumbas, E. Papantonopoulos and G. Siopsis, JHEP **0805**, 107 (2008) [arXiv:0801.4921 [hep-th]].
- [17] J. P. S. Lemos, Phys. Lett. B **353**, 46 (1995).
- [18] L. Vanzo, Phys. Rev. D **56**, 6475 (1997).
- [19] D. R. Brill, J. Louko and P. Peldan, Phys. Rev. D **56**, 3600 (1997).
- [20] Y. S. Myung, Phys. Lett. B **645**, 369 (2007).
- [21] D. Birmingham and S. Mokhtari, Phys. Rev. D **76**, 124039 (2007) [arXiv:0709.2388 [hep-th]].
- [22] M. Nadalini, L. Vanzo and S. Zerbini, Phys. Rev. D **77**, 024047 (2008) [arXiv:0710.2474 [hep-th]].
- [23] S. W. Hawking and D. N. Page, Commun. Math. Phys. **87**, 577 (1983).
- [24] Y. S. Myung, Y. W. Kim and Y. J. Park, Phys. Rev. D **78**, 084002 (2008) [arXiv:0805.0187 [gr-qc]].
- [25] B. H. Lee, S. Nam, D. W. Pang and C. Park, Phys. Rev. D **83** (2011) 066005 [arXiv:1006.0779 [hep-th]].
- [26] G. T. Horowitz and M. M. Roberts, JHEP **0911**, 015 (2009) [arXiv:0908.3677 [hep-th]].
- [27] R. A. Konoplya and A. Zhidenko, Phys. Lett. B **686**, 199 (2010) [arXiv:0909.2138 [hep-th]].